Microelectronic Engineering 86 (2009) 573–576

Contents lists available at ScienceDirect

Microelectronic Engineering

journal homepage: www.elsevier.com/locate/mee

Interferential lithography of 1D thin metallic sinusoidal gratings: Accurate control of the profile for azimuthal angular dependent plasmonic effects and applications

Filippo Romanato [a,b,c], Husen Kartasasmita Kang [a,*], Kwang Hong Lee [a], Gianluca Ruffato [b], Mauro Prasciolu [c], Chee Cheong Wong [a]

[a] School of Materials Science and Engineering, Nanyang Technological University, Block N4.1 - Nanyang Avenue, Singapore 639798, Singapore
[b] Department of Physics, University of Padova, via Marzolo 8, Padova 35131, Italy
[c] CNR-INFM TASC National Laboratory, Basovizza 34012, Trieste, Italy

ARTICLE INFO

Article history:
Received 29 September 2008
Received in revised form 6 January 2009
Accepted 16 January 2009
Available online 7 February 2009

Keywords:
Interference lithography
Plasmonic crystals
Gratings
Simulation

ABSTRACT

Nonlinear processes involved in the manufacture of nominally sinusoidal surface relief diffraction gratings generated by interference lithography can introduce distortions into the profile of these surfaces. Such distortions may dramatically affect both the specular reflectivity and diffracted efficiencies from such a surface [H. Raether, Phys. Thin Film 9 (1977) 145–261]. We shall consider in particular the case of metallic gratings used to investigate plasmonic effects that can be engineered for bio-sensing applications. To investigate these effects, interference lithography (IL) has been used for the generation of profile controlled sinusoidal plasmonic crystals. IL exposure contrast study has been performed to control the amplitude oscillation and the surface roughness quality. Bi-metallic layer of silver and gold have been systematically deposited with different film thicknesses. A comprehensive numerical model that studies the optical coupling to surface plasmon polaritons on Ag/Au gratings has been undertaken for the simulation of the reflectivity and azimuthal angle dependence [Z. Chen, I.R. Hooper, J.R. Sambles, J. Opt. A: Pure Appl. Opt. 10 (1) (2008) 015007]. This computation illustrates the sensitivity of individual features to specific harmonic components of the surface, for surface plasmon resonances recorded in both the zeroth and higher diffracted orders. The roughness surface control after development and after bi-metallic evaporation strongly contributes to tighten the width of the reflectivity peak. Optimization process has shown that for an Ag (37 nm) and Au (7 nm) metallic bilayer, a semi-amplitude of 20 nm provides the best reflectivity.

1. Introduction

Surface plasmon resonance (SPR) is an optical phenomenon in which free electrons are oscillating inside a metal surface when the frequency of SPR is coincident with the incident electromagnetic waves. This wave is also referred as to surface plasmon polariton (SPP) and it originates from coupled oscillations of electromagnetic field and density of electron plasma on a metallic surface [1–3].

The presence of SPP is recognizable by the sharp dip in the reflectivity curve; this optical response has become a widespread ultrasensitive tool for sensing purposes. Surface plasmons can be excited either using higher refractive index medium, or in our case, by a periodic structure (i.e. plasmonic grating) [4,5]. The extremely sensitive optical responses of gratings are greatly affected by geometrical parameters of the corrugated metallic film and multi-layer materials properties such as periodicity (lateral), amplitude (vertical), roughness and metals thickness [6,7].

In this paper, we would like to study the effects of each parameter both theoretically (by computer simulation) and experimentally in order to optimize them and obtain the sharpest and deepest reflectivity curve. This would then represent the condition for maximum SPP coupling efficiency, and hence enhanced sensitivity. Experimentally, in order to investigate these geometrical effects, interference lithography (IL) is applied on Si substrate for the generation of finely controlled sinusoidal profile plasmonic crystals. IL offers the most economical and efficient way to produce 1D, 2D and 3D array of nanostructures for the plasmonic crystals. It also allows vast number of identical and highly uniform structures to be patterned over a large area with short cycle and simple setup [8–10]. The shape of various profiles can be confidently and speedily dealt with to optimize the geometrical parameters, i.e. amplitude, roughness and the metal thickness. Several models have also been simulated based on a full analytical model.

In this work, 1D sinusoidal plasmonic crystal of different periodicities and amplitudes fabricated by IL are deposited by

* Corresponding author. Tel.: +65 94604650; fax: +65 67909081.
E-mail address: husen@pmail.ntu.edu.sg (H.K. Kang).

0167-9317/$ - see front matter © 2009 Elsevier B.V. All rights reserved.
doi:10.1016/j.mee.2009.01.080

gold–silver bi-metallic layer. Silver is preferred because of its smaller extinction coefficient than gold and thus less coupling losses (higher plasmonic coupling efficiency). However a very thin gold coating is used to prevent silver's oxidation and provide an inert surface for bio functionalization. The Au–Ag bi-metallic layer is then aimed to obtain both stable and high performance plasmonic grating based sensors [11]. Comparing the enhancement fields of the two metals the optimum thickness of Ag has been determined. A careful control of the geometrical parameters has been obtained by varying the distance, exposure time and incident angle of the IL set-up. In particular a fine calibration of the lithographic process is allowed to control the optical responses of the grating amplitude as well as the surface roughness.

2. Experimental

2.1. Fabrication-IL set-up

Interference lithography has been performed using Lloyd's configuration (L shape bracket) [10]. This Lloyd holder is attached on a rotating stage with precision 0.01° in order to have a fine control of the periodicity over the sample. A 40 mW helium cadmium (HeCd) laser from KIMMON emitting a single TEM 00 mode at 325/441.6 nm, respectively is used as the source. The laser light has a 30 cm coherence length, sufficient to prevent phase changes after the beam expands from the spatial filter. The spatial filter allows high frequency noise to be removed from the beam to provide a clean Gaussian profile. It contains two main parts, namely, an objective lens and a pin hole. For the objective lens, we use UV objective lens with 27*x* magnification, numerical aperture (NA) = 0.13, focal length (*f*) = 5.77 mm and range of wavelength = 245–440 nm. The calculated size of pin hole is equal to 1.25 μm for d_{beam} = 3 mm. The mirror is coated with aluminum to enhance UV reflectivity over broad range of angle. Pair of metallic mirrors is used to direct the beam path and to allow for alignment. High flatness mirror is required to form uniform pattern and intensity over large area. The beam finally expands to a diameter of 0.4 m at the exposure stage, where it illuminates the substrate and a mirror perpendicular to the substrate. A high speed digital shutter is used to control the exposure period and to minimize pattern distortion during shutter transient.

Interference between the light coming from the spatial filter and its mirror image forms a standing wave pattern on the substrate. Analysis of the Lloyd's mirror system used for these experiments predicts that the modulation should be on the order of 0.9. Exposure uniformity and repeatability are very good in the center of the expanded beam, and the samples were small enough to fit into this region.

2.2. Experimental procedures

The Si wafer is preferred as substrate in this project due to higher flatness and opaqueness. The substrate is cut into 1 × 1 inch and cleaned using piranha solution for 20–30 min. The samples are rinsed in de-ionized water for 15 min and then dried in the oven at 120 °C for 10 min. Surfaces of many of the metals oxidize very easily and forms long range hydrogen bonds with water adsorbed from the air, causing poor adhesion. Hence prior to spin coating the substrates with photoresist, adhesion promoter (primer) is applied.

Photoresist S1805 (Microposit®, Shipley European Limited, UK) was used diluted in EC-solvent (Microposit®, Shipley European Limited, UK) in ratio of 2:3, in order to get an appropriate film thickness, in this case around 130 nm. The spinning rate is 5000 rpm for 30 s to achieve 130 nm film thickness as measured using a profilometer and ellipsometer (using *genocs* method) [12]. Soft bake was performed at 90 °C for 12 min. An antireflective coating (ARC, either Brewer Science XHRi-16 or AZ Barli) was used to minimize the back reflection into resist layer. The samples are put in Lloyd's bracket, exposed for different time and distance to get different height (amplitude). The grating constant is given by $\Lambda = \lambda/(2 \sin \theta)$. θ is the incidence angle of parallel laser beams with respect to the mirror. After development, the samples are evaporated with different thickness of Ag and finally covered by 7 nm of Au.

The laser power after adjustment should be larger than 5 mW/cm^2 as determined with a power meter in front of the 5 μm pinhole. The exposure time is given by the photoresist's sensitivity (threshold energy needed to fully harden/soften the resist, D_0 = 18 mJ/cm^2).

3. Result

3.1. Nanofabrication

The Lloyd's mirror angular position needs to be finely calibrated and controlled in order to obtain a precise lattice parameter. The lattice period measurements have been taken using both atomic force microscopy (AFM) and asymmetric reflectivity configuration based on first order of diffraction gratings, scanning from 15° to 80° with a step size of 0.5° by using a 75 W Xe lamp, monochromatized from 500 to 800 nm with a bandwidth of 2.7 nm. All measurements were acquired and processed using a J.A. Woollam Co. VASE instrument and software [12]. This method determines precisely the lattice parameter that plotted as a function of the Lloyds' incidence angle (Fig. 1). This calibration curve allows us to determine the angular offset and lattice parameter of the gratings with high precision. The AFM image of the high quality grating with periodicity of 470 nm is shown in the inset of Fig. 1.

Several set of samples with different periodicities i.e. 420, 435, 445 and 470 nm and amplitudes (15–90 nm) have been fabricated using IL method and they are evaporated by different thickness of Ag and covered by 7 nm of Au. The control of grating's geometry is very crucial to provide optimum plasmonic responses. Generally, the amplitude of the grating can be controlled by varying the dose modulation, exposure period, the distance from pin hole and the power of the incident beam. Long distances from pin hole is preferred in order to obtain larger uniform area to reduce non planar

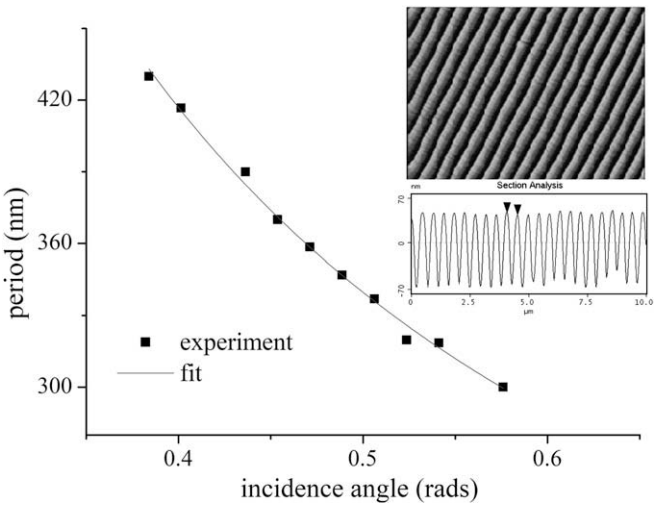

Fig. 1. Actual vs. calculated incident angle in Lloyds' system. In the inset is the AFM image of the grating produced from IL.

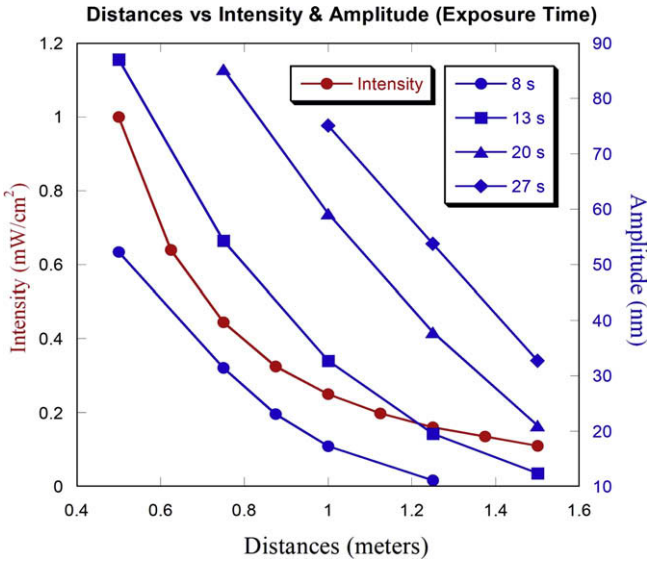

Fig. 2. The red line (left scale) is beam intensity (dose per unit time) measurement using power meter in front of sample stage as a function of exposure distance and the blue lines (right scale) are the amplitude measurements for different exposure times (doses) as a function of exposure distance. It can be observed from the graph that varying the exposure distances provide more severe effect in amplitude compared to the exposure time. However the exposure time is proportional to the grating amplitude for smaller amplitude for constant development time (60 s). (For interpretation of the references to colour in this figure legend, the reader is referred to the web version of this article.)

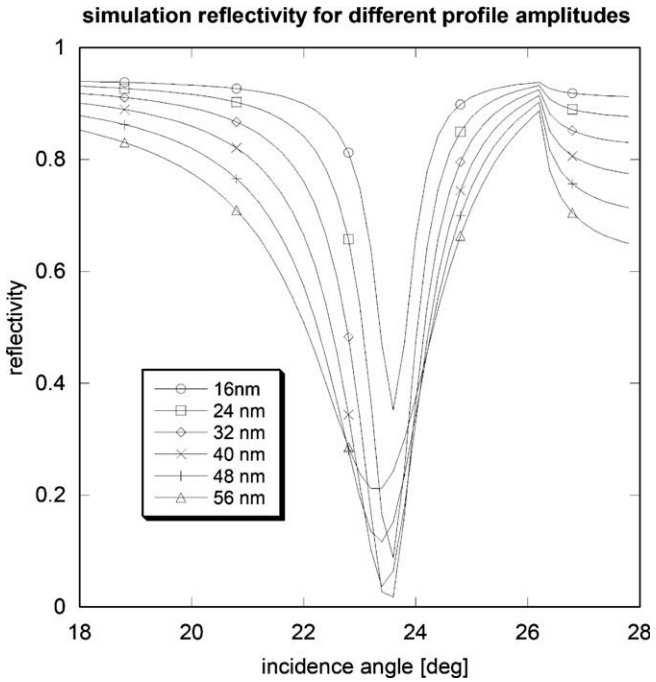

Fig. 3. Reflectivity spectrum of different grating amplitudes for 416 nm periodicity, evaporated with 37 nm of Ag and 7 nm of Au. It is shown that the best coupling efficiency (lowest dip) is performed by amplitude equals to 32 nm.

effects of the incident beam with the plane wave front, high control and stability over the exposure condition [10].

Fig. 2 shows the relations among the distances (radial of beam expansion), beam intensity and the amplitude of gratings for different exposure times at constant development time (60 s). As the exposure time is increased, the curves are getting linear (Fig. 2). It can also be observed that for longer distance i.e. 150 cm, the changes in amplitudes with respect to exposure time decrease by almost three times. In other words the amplitude has a slower rate compared to the one at shorter exposure distance therefore a better amplitude control can be achieved. The amplitude however will be limited by the minimum dose, d_{min} (not zero) which is resulted from interference of two beams. In order to get a full separation between lines gratings, high dose modulation is desired. It is where the bright fringes from the maximum intensity, I_{max} have enough time to penetrate through the resist thickness, D_0. Dose modulation will be reduced as the exposure distance increases; hence there will be a tradeoff between better control and maximum grating amplitude.

3.2. Simulations and characterizations

A simulation of SPP coupling on Ag–Au gratings is numerically done using an analytical model to solve Maxwell's equations in non-Cartesian system [13,14]. This simulation included the contribution of gratings' profile into the equations [15]. This simulation is calculated by comprehending the trends inherent in changing the parameters for a fabrication optimization. Several parameters are considered to be important namely: periodicity, amplitude, metal thickness and roughness.

The reflectivity spectrum of different sinusoidal grating amplitudes for 416 nm periodicity is shown in Fig. 3. There is a shifting in resonance angle toward higher value as the amplitude increases. It is necessary to optimize the amplitude in order to obtain the lowest reflectivity that can be experimentally done by fine exposure control. In this case, it is shown that the best coupling condition is performed by amplitude equal to 32 nm.

Fig. 4 shows the simulations of plasmon coupling efficiencies as a function of Ag thickness for different Au thickness and grating amplitudes while the periodicity is fixed. It appears from the figure that the optimum SPP coupling, represented by the deepest dip in the reflectivity curve, is shown by plasmonic gratings with Ag thicknesses ranging from 40 to 50 nm and amplitudes from 32 to 40 nm.

From the knowledge obtained from simulations and capability to control the geometries, three samples with periodicity of 416 nm and amplitude of 32 nm are fabricated to find the optimum silver thickness while the gold thickness is fixed as the simulation

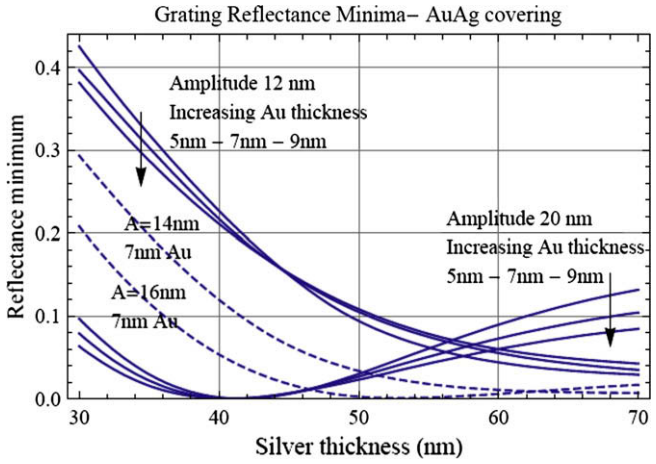

Fig. 4. Reflectance minima as a function of Ag thickness for different Au thicknesses (5, 7 and 9 nm) and grating amplitudes (12, 14, 16 and 20 nm). The amplitude values are equal to half peak-to-valley. The simulations show that the deepest reflectivity dips (perfect SPP coupling) is shown by plasmonic gratings with Ag thicknesses ranging from 40 to 50 nm and amplitudes from 32 to 40 nm.

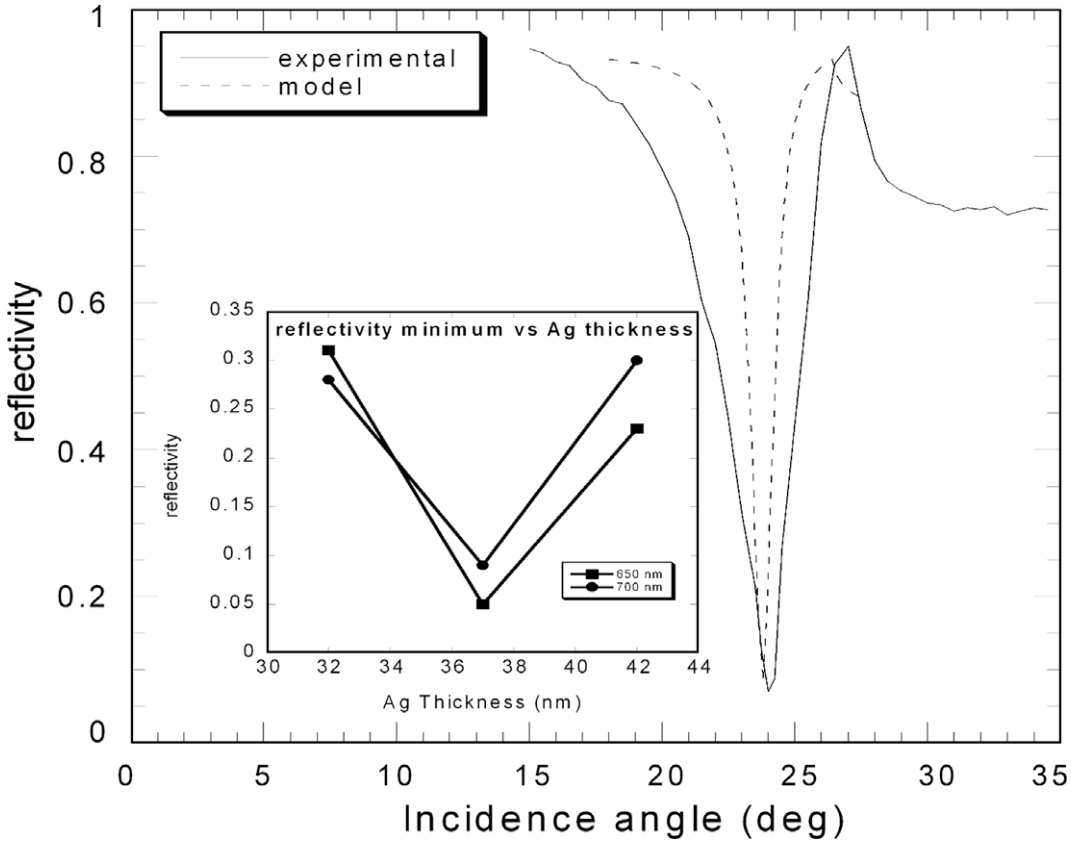

Fig. 5. Comparison between experimental and simulation (model) of reflectivity spectrum for identical geometrical parameters. It can be observed that the experimental measurement has broader reflection dip than the simulated one, indicating richer information. In other words, the roughness is not been fully included in the simulations. Inset is the experimental result of reflectivity vs. Ag thickness for different wavelength; while the periodicity and amplitude are fixed to be 500 nm and 32 nm, respectively. Reflectivity of optimized plasmonic crystal for periodicity 416 nm, amplitude 32 nm and 37 nm Ag and 7 nm Au, measured at 600 nm.

value (7 nm). These samples are characterized by the SPR system. Experimentally we have obtained a good agreement with the simulation results as can be confirmed by the reflectivity spectrum. The best coupling condition ($R = 5\%$) can be achieved when amplitude equals to 32 nm while optimum metal thicknesses are to 37 nm for Ag and 7 nm for Au (Fig. 5–inset).

There is some small discrepancy between the theoretical and experimental value for the metal thickness and amplitude. This is mainly due to difficulties of the model and geometrical parameters to accurately simulate the width and minimum dips of the experimental reflectivity spectrum (Fig. 5). Another factor that causes the discrepancy is surface roughness that severely affects the SPP coupling condition. The roughness of samples examined in this paper can be controlled down to 3–4 nm after the IL development. The simulation of the roughness effect is still under progress.

4. Conclusion

The geometrical effects of plasmonic crystal have been studied both experimentally by IL and theoretically (by simulation). Some parameters have been optimized in order to get the best coupling condition. There is a discrepancy between the experiment and simulation result which is mainly due to the roughness of the gratings.

References

[1] H. Raether, Physics of Thin Film 9 (1977) 145–261.
[2] Z. Chen, I.R. Hooper, J.R. Sambles, Journal of Optics A: Pure and Applied Optics 10 (1) (2008) 015007.
[3] Filippo Romanato, Lee Kwang Hong, Husen Kartasasmita Kang, Chee Cheong Wong, Zong Yun, Wolfgang Knoll, Physical Review B 77 (2008) 245435.
[4] E. Kretschmann, H. Raether, Zeitschrift für Naturforschung–Teil A: Physik, Physikalische Chemie, Kosmophysik 23 (1963) 2135–2136.
[5] H. Raether, Surface Plasmons on Smooth and Rough Surfaces and on Gratings, Springer-Verlag, Berlin, 1988.
[6] A.J. Ward, J.B. Pendry, Journal of Modern Optics 43 (4) (1996) 773–793.
[7] R. Petit, Electromagnetic Theory of Gratings, Springer, 1980.
[8] H.C. Guo, D. Nau, A. Radke, X.P. Zhang, J. Stodolka, X.L. Yang, S.G. Tikhodeev, N.A. Gippius, H. Giessen, Applied Physics B 81 (2–3) (2005).
[9] Maya Farhoud, Juan Ferrera, Anthony J. Lochtefeld, T.E. Murphy, Mark L. Schattenburg, J. Carter, C.A. Ross, Henry I. Smith, Journal Vacuum Science and Technology B 17 (6) (1999) 3182.
[10] Thomas B. O'Reilly, Henry I. Smith, Journal Vacuum Science and Technology B 26 (6) (2008) 2131–2134.
[11] Biow Hiem Ong, Xiaocong Yuan, Swee Chuan Tjin, Fiber and Integrated Optics 26 (4) (2007) 229–240.
[12] J.A. Woollam Co., I., Spectroscopic Ellipsometry–Data Acquisition and Analysis in A Guide to use WVASE 32. 2006.
[13] G.P. Bryan-Brown, M.C. Jory, S.J. Elston, J.R. Sambles, Journal of Modern Optics 40 (5) (1993) 959–964.
[14] J. Chandezon, G. Raoult, D. Maystre, Journal of Optics-Nouvelle Revue D Optique 11 (4) (1980) 235–241.
[15] G. Ruffato, Surface Plasmon Polaritons on 1D-Gratings, in: Department of Physics, University of Padova, Padova, 2008, p. 83.